Prediction Model of wave Propagation Inside Buildings Including Specular and Diffracted Transmission and Reflection

Seong-Cheol Kim* *Regular Member*

ABSTRACT

The growing use of unlicensed wireless systems has spurred interest in the 2.4 Ghz ISM band. In order to facilitate the efficient design of such systems, understandings of the properties of radio wave propagation in buildings is necessary. Many authors have reported about statistical propagation models based on the extensive measurements in buildings. However, measurement based statistical analysis will not be enough for the optimum deployment of the communication systems in the specific building. Avoiding expensive measurements in the individual buildings prior to installation, or adjustments afterwards, theoretical prediction models have been developed to predict the path loss and delay spread from the building floor plan. Predictions shows good agreements with measurements except for a few environments which was surrounded by heavy scatterers.

I. Introduction

UHF(300 MHz to 3 GHz) radio waves are the basis for modern wireless communication systems. Development and application of wireless communication systems in these bands requires the characterization of the wave propagation in various environments. Propagation inside buildings is of primary interest for wireless LAN and wireless PBX systems.

The modeling of wave propagation inside building is essential to the understanding of the characteristics of the indoor wireless communication channels. Measurements of CW and pulsed signals are the most common methods to model the radio channel. A few authors reported theoretical prediction models for indoor wave propagations in the 900 MHz and 1.8 GHz band using ray tracing techniques [1-3]. These studies have accounted for specular reflection and transmission properties at walls using reflection and transmission coefficients obtained theoretically or experimentally at 900 MHz.

In order to carry over the ray tracing techniques to permit theoretical prediction of radio wave propagation in the 2.4 GHz band, it is necessary to account for the diffraction grating effect at concrete block walls. As discussed in [4], the internal structure of webs and voids inside concrete blocks causes them to act as a diffraction gratings at high frequencies. As a result, ray incident on such a wall will give rise to reflected and transmitted diffraction orders of significant amplitude so that those must be traced as well as the specular rays.

In this study, two dimensional ray tracing methods was used to account for both specular and diffracted components of transmitted and reflected rays at concrete block walls. Despite the use of a two dimensional ray tracing technique, the prediction model can be considered as virtual three dimensional model by means of introducing the excess path loss concepts effectively taking into account the vertical spreading of the rays [1].

* AT&T Laboratories, Holmdel, New Jersey
論文番號:97320--0910
接受日字:1997年 9月 10日

Prediction results made with only specular components of the transmitted and reflected ray are compared to those obtained by the model that account for the diffraction orders. Comparisons show that diffracted rays induced by walls having periodic internal structures play an important role in determining the radio wave coverage inside buildings.

II. Overview of Wave Propagation in Buildings

As radio wave propagates away from the transmit antenna in free space, its intensity attenuates in inverse proportion to the square of propagation distance ($\sim 1/L^2$). This attenuation can be viewed in terms of the uniform spreading of the radiated rays in both the vertical and horizontal planes. If no obstacles are encountered, the cross section of a narrow tube filled with coherent rays is proportional to the square of distance from the source L^2 so that the signal intensity decreases in inverse proportion to the square of the distance L^2 to conserve radiated power. The conservation of power in the ray tube leads to find the field intensity of the ray that undergos grating diffraction at concrete block walls.

Ray spreadings in buildings are thought to be induced separately in the vertical and horizontal planes. Since the concrete blocks are composed of the webs and voids running vertically, the diffraction orders lie in the horizontal plane so that grating diffractions take place in the horizontal plane. This horizontal spreading effect is taken into account by tracing diffraction orders and specular components of the traveling rays in the two dimensional horizontal plane. When a ray is incident on regular walls, only specular reflection and transmission takes place, leading to a binary tree structure of ray tracing. In this case the horizontal spreading of the ray tube is proportional to the total unfolded path length. However, a ray incident on walls having periodic internal structures induces diffracted transmissions and reflections as well as specular ones, which result in a m-ary tree (multi-children tree) structure of ray tracing. The diffraction orders of the transmitted or reflected rays are to have complex analytical forms.

Within a room, radio waves propagate through the clear space between the ceiling and furniture. Ceilings, metal beams supporting the roof, utility pipes, lighting fixtures, etc. limit the upper boundary of the clear space since they scatter the incident radio wave into all directions. The lower limit of the clear space is defined by the furniture on the floor such as desks, cabinets, shelves, movable partitions, as well as people. The width of the clear space ranges from 1.5 to 2.5 meters in a common office building and the storage room of a large retail store, while it ranges from 3 to 4 meters in the sales floor of retail stores. The obstacles that determine the clear space scatter radio waves incident upon them to give rise to an excess path loss, which increase sharply with propagation distance. The excess path loss can be computed by assuming the scattering obstacles as a series of absorbing screens. Kirchhoff-Huygens diffraction theory is then used to compute the field propagating past successive pairs of absorbing screens. The excess path loss is obtained by normalizing the field strength of the ray after propagating through pairs of absorbing screens to that of the ray that has traveled the same distance through the free space. The irregularity of the upper and lower boundary of the clear space and randomness of the moving people cause the signal at the receiver to be stochastic processes. The spatial randomness induced by scatterers can be eliminated by taking the sector average over several wavelengths [5].

The accurate prediction of the wave propagation in buildings can be obtained by adding up all the possible losses. The first possible loss is free space path loss being proportional to $1/L^2$. The second is the excess path loss in the vertical plane, which depends on the clear space between the upper and lower boundary. The last is the loss in the horizontal plane, which is caused by the transmission and the reflection at walls.

III. Excess Path Loss in Vertical Plane

As a ray propagate, it spreads in the vertical and the horizontal plane. In the vertical plane, obstacles such as the ceiling structure, the furniture and moving people affect the vertical spreading and cause the excess path loss. Assuming those obstacles as a series of absorbing screens as shown in Figure 1, the excess path loss can be obtained by the theoretical model developed by Honcharenko and Bertoni[1].

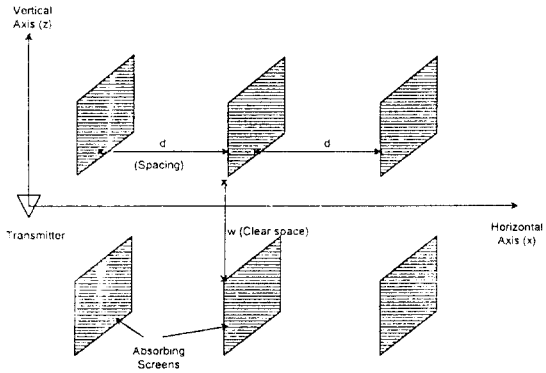

Fig. 1 Absorbing screens model for obstacles limiting clear space in the vertical plane

In Figure 1, d is spacing between adjacent absorbing screens and w is the aperture between the upper and lower absorbing screens. The vertical axis is designated as the variable z, and the horizontal axis as the variable x. Considering only the vertical spreading, the transmitter is assumed to be a line current source locating in the middle of the clear space. The field radiated by the line current source can be expressed as

$$H = \frac{e^{-jkr}}{\sqrt{kr}} \tag{1}$$

where k is the wave number and r is the distance between the source and the observation point. In order to consider the randomness of the lower and the upper boundaries of the clear space, the aperture size w is taken to be a uniformly distributed random variable varying between the maximum and minimum aperture. The field strength in the nearest aperture to the transmitter is given by equation (1). According to Kirchhoff diffraction theory [6], the field at the second aperture is the superposition of the fields induced by the equivalent line sources in the first aperture. Similarly, the fields in the $(m+1)^{th}$ aperture are excited by the equivalent line source in the m^{th} aperture. These deduction can be applied recursively in order to obtain the field strength in an arbitrary aperture. The mathematical expression for the recursive interaction process [7] is given by

$$H_{m+1}(z) = \frac{e^{j\pi/4}}{2\sqrt{\lambda}} \int_{-w/2}^{w/2} H_m(z') \frac{e^{-jkr}}{\sqrt{r}} (1+\cos\alpha) dz' \tag{2}$$

$$r = \sqrt{d^2 + (z-z')^2} \tag{3}$$

$$\cos\alpha = \frac{d}{r} \tag{4}$$

where d is distance between adjacent apertures and λ is the wave length of the light in the free space, while z and z' are the vertical positions of the observation point and the source point, respectively.

The excess path loss is obtained in the following procedures. First, the square of the field strength $H_m(z)$ at the m^{th} aperture is calculated by equation (2). Average of $|H_m(z)|^2$ is taken over z which varies between -w/2 and w/2. The excess path loss at a distances $L = md$ is then obtained by normalizing the $|H_m|^2$ to $1/kL$, which is the square of the filed strength in free space at distance L from the line source. Finally, polynomial curve fitting is applied to the discrete excess path loss in order to obtain a continuous excess path loss curve. The continuous excess path loss curves at 2.4 GHz for the apertures whose size vary randomly between 1.5 and 1.4 meters and between 2 and 2.5 meters are shown in Figure 2.

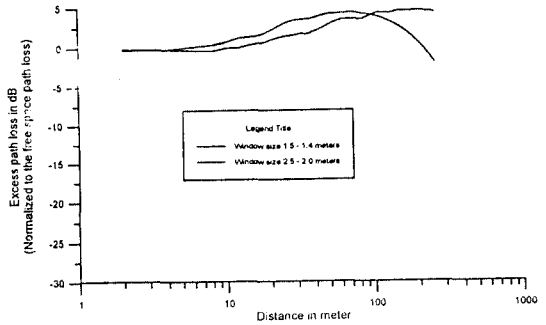

Fig. 2 The excess path loss curves at 2.4 GHz

IV. Horizontal spreading of the ray

In order to account for horizontal spreading effect of the ray on the radio propagation in buildings, two dimensional ray tracing technique in the horizontal plane is used. Radiation from the transmit antenna is modeled as sum of adjacent rays equally angular spaced on the azimuthal plane assuming ray optics. The behavior of these rays is approximated by tracing individual rays leaving the source with the same angular spacing in the horizontal plane, which in this study is 2 degree or less. The rays are individually traced in the horizontal plane until the power being carried by each ray attenuates to any given threshold level. When the ray encounters a wall, rays are transmitted and reflected off the wall both in the specular direction as well as in grating diffraction order directions. Noticing that most of interior walls in this study satisfy the "Rayleigh criterion"[8], diffusive scattering can be ignored. The properties of the reflection and the transmission at the wall are determined by the internal structure of the wall.

For specular transmission, the ray propagates off the wall in the same direction as the incident ray, and the angular spacing between adjacent rays remains unchanged as shown in Figure 3(a). Specular reflection has the same properties as the specular transmission except that the direction of the reflected ray is the mirror image of the transmitted ray with respect to the wall. This implies that specular transmission or

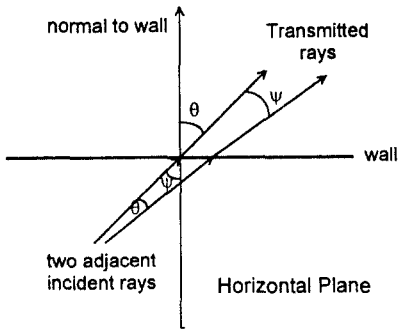

(a) Specular transmission

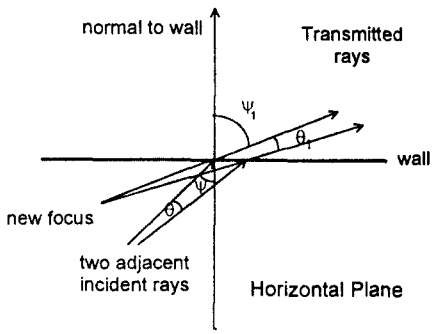

(b) Diffracted transmission

Fig. 3 Schematic diagram of the specular and diffracted transmission at the wall

reflection on the wall does not change the spreading properties in the horizontal plane. Analogy can be deduced for the spreading properties in the vertical plane since the electromagnetic porperties of the interior walls are assumed to be homogeneous in the vertical plane. In case of grating diffraction order transmission as shown in Figure 3(b), the transmission angle Ψ_1 with respect to the normal to the wall differs from the incident angle Ψ in order to satisfy the boundary condition at the wall[4]. In addition, the angular spcaing θ_1 after transmission is different from the angular spreading of the incident ray θ [9]. Corresponding statements hold for the diffracted reflection. However, spreading in the vertical plane is

unchanged by the diffraction in the horizontal plane. The difference of the spreading properties in the two orthogonal planes produces an astigmatic virtual focus for the diffracted rays.

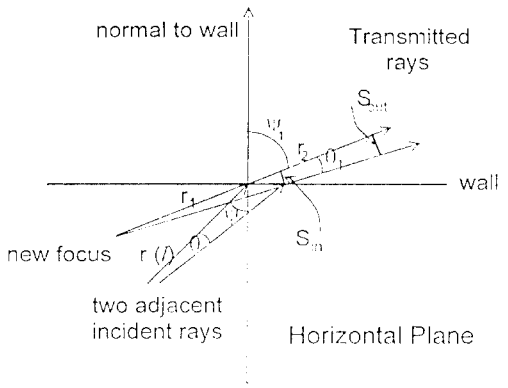

Fig. 4 Relationship between the incident and the grating diffracted rays

The relationship between the power intensity and the angular spacing of the rays before and after transmission or reflection can be explained schematically by referring to Figure 4. As shown in Figure 4, r is the distance to the point of incidence from the actual focus of the ray tube incident on the wall, and r_1 is the distance from the virtual focus of the diffracted ray tube to the incident point. The l is the unfolded distance along the ray path from the transmitter to the wall. In other words, it is the distance to the point of incidence from the focal point in the vertical plane of the ray tube. r_2 is the distance along the ray path from the wall to the observation point. As discussed in [4], the incident and the transmitted angles are coupled by the following equation,

$$\sin \Psi + m \frac{2\pi}{kp} = \sin \Psi_1 \tag{5}$$

where m is the diffraction order and p is the periodicity. For small angular spacing between adjacent rays θ, the angular spacing after diffracted transmission θ_1 can be obtained by differentiating both sides of equation (5),

$$\cos \Psi d\Psi = \cos \Psi_1 d\Psi_1 \tag{6}$$

where $d\Psi$ and $d\Psi_1$ implies θ and θ_1, respectively. Therefore θ_1 is represented by

$$\theta_1 = \theta \frac{\cos \Psi}{\cos \Psi_1} \tag{7}$$

The vertical focal distance r_1 can be found considering the fact that the projection of both the incident ray tube and the equivalent ray tube having a new focus on the wall must be same in order to satisfy the power conservation law,

$$\frac{r\theta}{\cos \Psi} = \frac{r_1 \theta_1}{\cos \Psi_1} \tag{8}$$

Combining equations (7) and (8), we have

$$r_1 = r \left(\frac{\cos \Psi_1}{\cos \Psi} \right)^2 \tag{9}$$

Let S_{in} and S_{out} be the input and output power intensities right after the wall and at a distance r_2 past the wall, respectively. Conservation of total power in the ray tube requires that

$$S_{out}(r_1 + r_2)\theta_1(l + r_2)\delta = S_{in} r_1 \theta_1 l\delta \tag{10}$$

where δ is the spreading angle in the vertical plane. The vertical spreading angle is the same for the incident and the diffracted rays. Thus we have that

$$S_{out} = S_{in} \frac{r_1 l}{[r_1 + r_2(l + r_2)]} \tag{11}$$

If $T_n(\Psi)$ is the transmission coefficient at nth wall, then S_{in} is equal to the product of $|T_n(\Psi)|^2$ and the

intensity of the incident ray field at the wall. Letting P_t be the effective radiation power of the transmitter, and accounting for all the previous transmission and reflection coefficients T_n and Γ_n, respectively, Sin is given by

$$S_{in} = \frac{P_t}{4\pi} \frac{1}{rl} \prod_m |T_m(\Psi_m)|^2 \prod_n |\Gamma_n(\Psi_n)|^2 \quad (12)$$

where the product are taken over all the transmissions and reflections undergone by the ray. Taking Z_0 to be the free space characteristic impedance and representing the excess path loss by $Ex(l)$, the electric field E at the distance r_2 along the diffracted ray path is found from

$$|E|^2 = \frac{Z_0 P_t}{4\pi} R(r_1, r_2; r, l) \prod_m |T_m(\Psi_m)|^2 \prod_n |\Gamma_n(\Psi_n)|^2 \quad (13)$$

where

$$R(r_1, r_2; r, l) = \frac{rl}{(r_1 + r_2)(l + r_2)} Ex(l + r_2) \quad (14)$$

The foregoing expressions give a way to compute the field along an individual ray path by tracing the angular spreading between adjacent rays, the cumulative propagation distance l and the virtual focus distance r as the ray undergoes multiple reflections and transmissions. The next section describes such a computer based ray tracing approach.

V. Ray tracing

Ray tracing is an effective methods to predict the CW receive power or the impulse response parameter theoretically. As explained in section 2, wave propagation in three dimension can be considered separately in the two orthogonal planes. The vertical spreading effect is well described by the excess path loss model even though it is negligible in this study. Hence it is only necessary to trace, in the horizontal plane, a series of rays with equal angular spacing that originate from the transmitter. As each ray propagates in the horizontal plane, it encounters several walls with different transmission and reflection properties as shown in Figure 5.

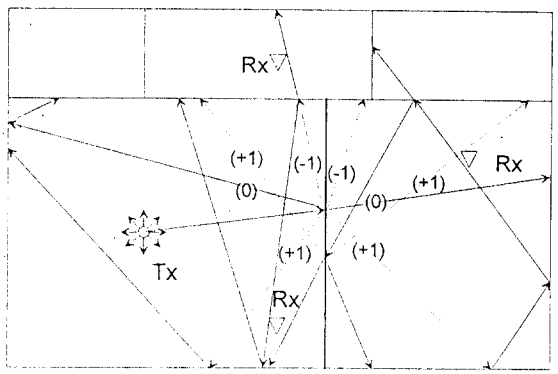

Fig. 5 Schematic diagram of the ray tracing

Whenever a ray encounters a wall, it generates two or more rays depending on the internal structure of the wall. The ray leaving the wall suffers power loss given by either the transmission or the reflection coefficient, in addition to the change of the horizontal spreading. In the ray tracing program, the ray retains its prior history, such as the accumulated path loss including the free space propagation loss and wall transmission and reflection loss at each wall encountered by the ray, the effective angular spacing between adjacent rays, the accumulated virtual focal distance, the actual travel distance and the number of walls that the ray have met, etc. During tracing the ray, the computer program checks whether the propagating ray hits any receivers in the room where the ray is currently located. Once the ray is captured by the receiver, the receive power carried by the ray and the propagation delay, which is obtained from the actual travel distance, are calculated to save in a output file. In order to determine if the ray illuminates a particular receiver, it is necessary to assign a finite width to the ray, or to the receiver. The logic for this is suggested in Figure 6. The rays ra-

diated by the transmitter are assumed to be equally distributed on the azimuthal plane with angular apacing of θ. Hence each ray can be viewed as covering a cross section, which for specular transmission and reflection has the width of $\theta(r+r_2)$ at the receiver point. For a diffracted path, the angular width is θ_1 and the distance to the virtual focus is r_1+r_2. Thus the width of the ray cross section at the receiver point is $\theta_1(r_1+r_2)$. The receiver is treated as illuminated by the ray provided that the length of the perpendicular projection of the receiver point onto the ray is less than the distance $d = \theta_1(r_1+r_2)/2$.

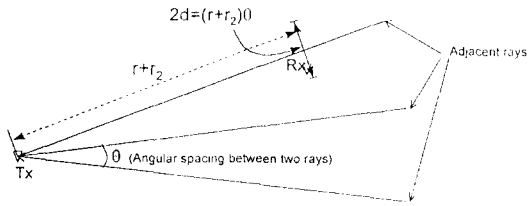

Fig. 6 Definition of the capture width of the ray

As the signal at the receiver is assumed to be random processes in time and in space [10], the amplitude and the phase of the received signal are random variables in space. Hence the total power for the CW excitation at the receiver is the coherent superposition of all the multipath rays, which is given by

$$E_r = \sum_i |E_i| e^{-j\phi_i} \tag{15}$$

Moving the receiver over several wavelengths, which is very small compared with the propagation distance, the amplitude of the field $|E_i|$ will be nearly constant, as shown in equation (13). However the phase φ_i can change by more than 2π, since the phase is the product of the displacement, whose length is l_i, and the wave number of the radio wave, which is $2\pi/\lambda$. Therefore, neglecting time variation, the expectation value of the total receive power can be represented by

$$\begin{aligned} \langle |E_r|^2 \rangle &= \left\langle \left| \sum_i |E_i| e^{-j\phi_i} \right|^2 \right\rangle \\ &= \sum_i \sum_k |E_i||E_k| \langle e^{-j(\phi_i - \phi_k)} \rangle \\ &= \sum_i |E_i|^2 \end{aligned} \tag{16}$$

In other words, the incoherent superposition of all the individual ray power is approximately the sector averaged receive power. It has been shown [5] that the expectation for $i \neq k$ in equation (16) vanishes when averaging is carried out over both the receiver and source position.

VI. Results and Discussion

A ray tracing program was written to embody the foregoing concepts, including grating diffraction at concrete block walls. The program was tested on the virtual building shown in Figure 7. Except one concrete block wall in the middle of the floor, all the other walls are assumed as artificial invisible walls, whcih allow total transmission of the incident ray. In order to investigate the generation of the grating diffracted rays, two tests were carried out. All the input parameters, such as the input file for the building, wall coefficients, and the angular space between adjacent rays at the source, were identical. In the first test, a single ray incident on the concrete at zero degrees relative to the normal was found to split into one specular and two diffracted rays. The specular transmitted ray illuminated the receiver 23 with a receive power of -82.6 dB. The diffracted ray of -1 order illuminated the receiver 1 with a receive power of -85.1 dB and the receiver 2 with a receive power of -85.08 dB. The diffracted ray of +1 order gave the mirrored results of the -1 order.

The second test was carried out with a incidence angle of -10 degree relative to the normal to the concrete block wall. In this test, the specular component illuminated the receiver 19 with a receive power of -82.4 dB and the diffracted ray of the +1 diffraction order illuminated receivers 34 and 35 with receive powers of -78.9 and -79.18 dB, respectively.

These tests show that the ray tracing program generated and traced the specular and the diffracted rays as the theory predicts.

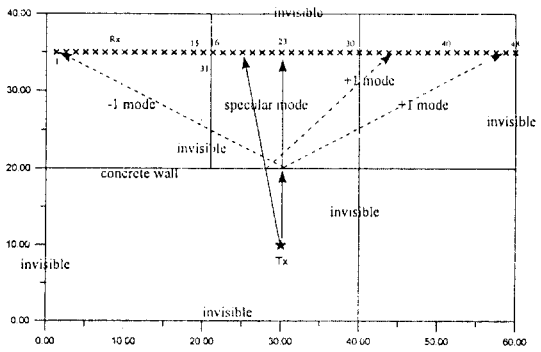

Fig. 7 Test of the grating diffraction properties of the ray tracing program

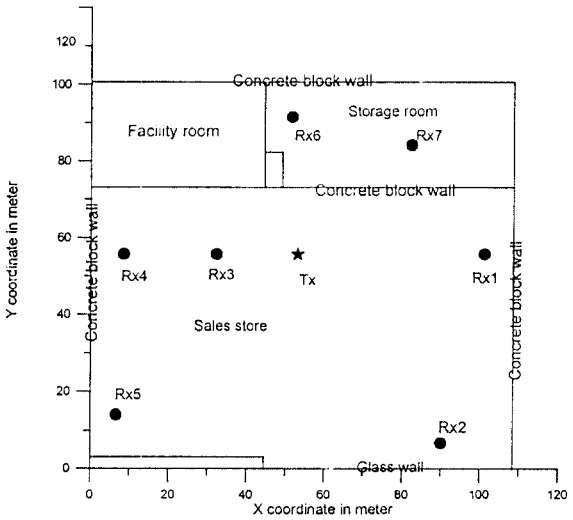

Fig. 8 Floor plan of the building used for ray tracing

The ray tracing program was applied to the retail store, where the CW path loss and the impulse response parameters were measured[12]. The floor plan is shown in Figure 8. Except for a glass wall at the entrance to the store, the exterior and interior walls are constructed of concrete blocks. The receivers located on the sales floor are illuminated by the transmitter without being blocked by any wall, even though the line of sight path is blocked by merchandise shelves. As a result many grating diffraction paths may exist between the receivers in the sales floor and transmitter. There is a concrete block wall between the receiver R×7 and the transmitter and a wooden door between the receiver R×6 and the transmitter.

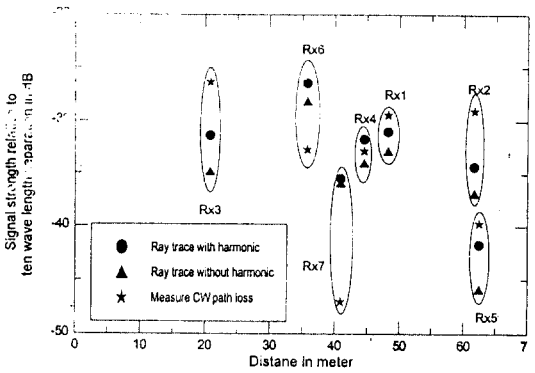

Fig. 9 Comparison between the measured and calculated CW path loss

Figure 9 compares CW path loss results obtained from the measurements and the prediction results by the ray tracing program that accounts for the grating diffraction orders at the concrete block walls as well as that ignores the diffracted rays. In general the ray tracing program that considers grating diffraction at the wall produce results closer to the measurements than the program that ignores diffraction. At receiver sites R×6 and R×7 the ray tracing program overestimates the receive powers, since the receivers are in heavily cluttered environments that cannot be accounted for by the program. If the extraordinary receiver site R×7 is excluded, the comparison shows that the ray tracing program including diffractions gives predictions of the CW path loss having an average error of 1.09 dB and a standard deviation of 3.92 dB.

By comparing path losses calculated by the ray tracing program in the frequency bands of 2.4 GHz and 900 MHz, the characteristics of the spatial coverage of the base station in two different frequency bands can be understood clearly. Figure 10 and Figure 11 show the contour plots of path losses in the sales

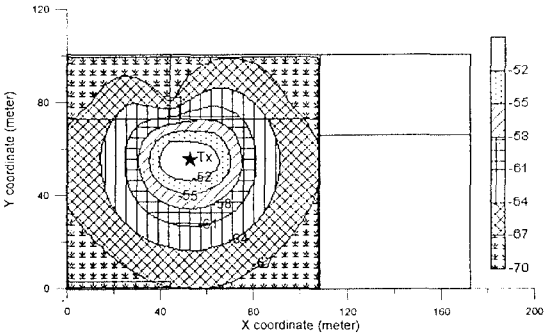

Fig. 10 Contour plot of path losses calculated by the ray tracing program considering the grating diffractions at 2.4 GHz

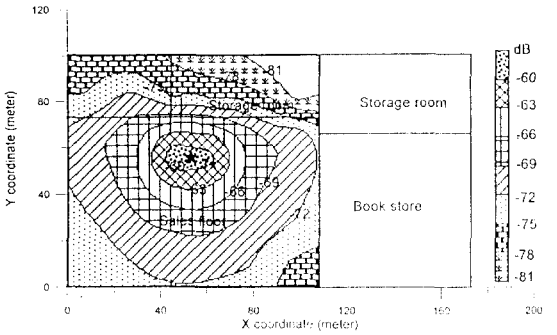

Fig. 11 Contour plot of path losses calculated by the ray tracing program at 900 MHz

floor at 2.4 GHz and 900 MHz, respectively. It is observed from two figures that the spatial coverage of the base station in 2.4 GHz is more uniform and less gradient than in 900 MHz. The shape of the coverage in 900 MHz looks circular, even though it is distorted near the concrete block wall between the sales floor and the storage room. The shape of the coverage in 2.4 GHz is irregular and seems to have something to do with the concrete block wall. These results can be explained by the fact that the concrete block wall generates the grating diffraction orders in high frequencies which carry significant amount of powers compared with the specular components for a certain incident angles at the concrete block wall having periodic internal structure.

VII. Conclusion

Wave propagation inside buildings can be explained by the ray optic methods. The excess path loss due to the vertical spreading can be evaluated using the concept of the clear space[1]. The horizontal spreading is accounted for by tracing the equally spaced individual rays in the horizontal plane. In the ray tracing it is necessary to account for the change of the ray propagation direction and the width of the ray tube for the grating diffraction orders generated at concrete block walls. Comparison of the measured results and the predicted results show good agreement except one extraordinary receiver site. Also the comparison tells us that the grating diffraction on the wall plays an important role in the ray tracing model. In addition, comparing the calculated path loss in two different frequencies, we can understand the characteristics of the base station coverage clearly.

Reference

1. W. Honcharenko, H. L. Bertoni, J. L. Dailing, J. Qian, and H. D. Yee, "Mechanism governing UHF propagation on single floors in modern office buildings," *IEEE Transactions on Vehicular Technology*, Vol. 41, No. 4, pp. 496-504, November 1992.
2. S. Y. Seidel and T. S. Rappaport, "Site-specific propagation prediction for wireless in-building personal communication system design," *IEEE Transactions on Vehicular Technology*, Vol. 43, No. 4, pp. 879-891, November 1994.
3. J. W. McKown and R. L. Hamilton, "Ray tracing as a design tool for wireless networks," *IEEE Network Magazine*, Vol. 5, No. 6, pp. 27-30., November, 1991.
4. W. Honcharenko and H. L. Bertoni, "Transmission and Reflection Characteristics at Concrete Blok Walls in UHF Band Proposed for Future PCS," *IEEE Transactions on Antennas and Propagation*, Vol. 42, No. 2, pp. 232-239, May 1994.

5. W. Honcharenko, H. L. Bertoni and J. L. Dailing, "Bilateral averaging over receiving and transmitting areas for accurate measurements of sector average signal strength inside buildings," *IEEE Transactions on Antennas and Propagation*, Vol. 43, No. 5, pp. 508-512, May 1995.
6. M. Born and E. Wolf, *Principles of Optics-Electromagnetic Theory of Propagation Interference and Diffraction of Light*. New York:Pergamon Press, 1989, pp. 370-382.
7. H. L. Bertoni and J. Walfish, "Theoretical model of UHF propagation in urban environments," *IEEE Transactions on Antennas and Propagation*, Vol. AP-36, No. 12, pp. 1788-1796, December 1988.
8. P. Beckmann and A. Spizzichino, *The Scattering of Electromagnetic Waves from Rough Surfaces*. New York:The Macmillan Company, 1963, pp. 9-16.
9. H. L. Bertoni and A. Hessel, "Ray optics for radiation problems in anisotropic regions with boundaries. II. Point-source excitation," *Radio Science*, Vol. 2, No. 8, pp. 793-812, August 1967.
10. J. G. Proakis, *Digital Communications*. New York: McGraw-Hill, 1989, pp. 702-719.
11. L. B. Felsen and N. Marcuvitz, *Radiation and Scattering of Waves*. New Jersey:Prentice-Hall, Inc. 1973, pp. 630-663.
12. S.C. Kim, H.L.Bertoni and M. Stern, "Pulse Propagation Characteristics at 2.4 GHz Inside Buildings," *IEEE Transactions on Vehicular Technology*, Vol. 45, No. 3, pp. 579-592, August 1996.

Seong-Cheol Kim

Seong-Cheol Kim was born in Taegu, Korea, on May 16, 1961. He received the B.S. and M.S. degrees in Electrical Engineering from Seoul National University, Seoul, in 1984 and 1987, respectively. He was awarded the Ph.D. degree in Electrical Engineering from the Polytechnic University, Brooklyn, NY in 1995.

From 1985 to 1987 he was a research assistant in the Plasma Engineering Laboratories in the EE Department at Seoul National University. Since 1991 he has worked for Center for Advanced Technology in Telecommunications at Polytechnic University with a grant from Symbol Technologies, Inc. From 1992 to 1994, he carried out experiments on the characterization of the indoor CW and pulsed radio propagation at Symbol Technologies, Inc., Bohemia, NY. He is now in the Special Study Division at AT&T Laboratories, Holmdel, NJ.

His research interests covers the characterization and modeling of communication channels, communication system performance analysis, propagation modeling of radio waves in buildings and urban environments, wireless communication system design including cellular, PCS and wireless LAN systems, RF communication through power line and electromagnetic theory. He has authored or co-authored over 10 journal and conference papers.

Dr. Kim was a student member of IEEE from 1991-1995. He is now a member of the IEEE and of Eta Kappa Nu. He also has served as the current president of Korean Scientists and Engineers Association New Jersey Chapter and served as 솥 conference chair of KSEA North-East Regional Conference 1998.